Research Project Report
Marshall Plan Fellowship

Development of Bioorthogonal Reactions and their Application in Targeted Cancer Therapy

Conducted by
DI Stefan Kronister

Vienna University of Technology

at the Massachusetts General Hospital/Harvard Medical School

in the research group of PhD Miles Miller

07.2018-12.2018

Contents

1. Introduction

More than 300.000 people are suffering from cancer in Austria and this number will be increased to 400.000 in 2022. One main issue of cancer therapy still is that common cancer therapeutics cannot differentiate between healthy and tumor tissue. Extensive efforts have been made to develop targeted cancer therapeutics. However, each of these various targeting strategies (antibodies, nanoparticles, ligands etc.) is subject to limitations and drawbacks.

The aim of this research project is to combine two different targeting strategies through bioorthogonal chemistry. Hence, limitations of each single targeting strategy can be overcome to enable cancer therapies with less off-target toxicity.

1.1 Bioorthogonal Chemistry – "Chemistry for human in human"

In contrast to common chemical reactions, bioorthogonal reactions can proceed within the molecularly complex and uncontrolled environment of living systems (Fig. 1).[1]
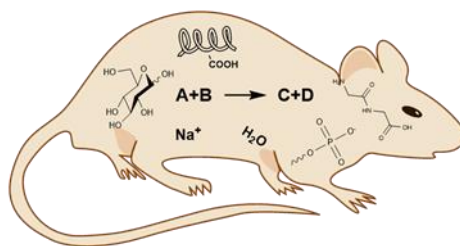
✔ highly selective reactions
✔ very fast reactions
✔ non-toxic
✔ biocompatible (aqueous media, etc)

Figure 1: Advantages of Bioorthogonal Chemistry

To fulfill these high requirements bioorthogonal reactions must meet some prerequisites:

➢ „Bio-inertness":	the functionalities involved in a bioorthogonal reaction and the resulting products must be metabolically stable in their applied biological environment
➢ Selectivity:	highly selective transformation between bioorthogonal reaction pairs avoiding any side reactions with molecules of the surrounding biological system
➢ High Reaction rates	fast kinetics even with low reactant concentrations in a physiological environment (pH and T)

1.2 Historical background of biorthogonal reactions

The first example of a bioorthogonal reactions among completely abiotic functionalities is the Staudinger Ligation enabling the formation of an amide bond via reaction between azides and phosphines (Fig. 2a). In spite of the considerable selectivity and biocompatibility in organisms, this prominent reaction has very low reaction rates ($k_2 \sim 10^{-3}$ M^{-1} s^{-1})[2] and the phosphine reagents are susceptible to oxidation by air or enzymes.[3]

Inspired by natures minimalistic and at the same time highly efficient synthetic approach towards bond formation reactions (i.e. highly complex biomolecules from repetitive addition of small building blocks), Barry Sharpless defined the pioneering concept of click chemistry.[4] Based on the Huisgen 1,3-dipolar cycloaddition between terminal alkynes and azides, he developed the first "click reaction" by adding Cu(I) as catalyst (Copper catalysed Azide-Alkyne Cycloaddition CuAAC, Fig. 2b).[5] As a result, the reaction rates increased and site specify of the cycloaddition was achieved. A major advantage of this approach is the use of an excellent bioorthogonal reaction pair (both azides and alkynes are abiotic) and the facile introduction of azides (via S_N or diazotation) in biomolecules. The cytotoxicity of Cu(I) (attributed to oxidative stress and Cu(I) mediated generation of reactive oxygen species) excludes its application from living systems.

To address this challenge, scientists developed Cu(I)-stabilizing ligands, circumvented Cu(I) by testing other transition metals and attempted to avoid it completely. Finally, Bertozzi and coworkers successfully modified the system by introducing ring strain in the alkyne-component to lower the activation energy and hence enable an acceleration without transition metals ("copper free click chemistry"). In spite of reaching a 1000-fold improvement compared to the classic Staudinger ligation, the strain-promoted azide-alkyne cycloaddition[6] (SPAAC, Fig. 2c) cannot compete with the rates of Cu(I) catalyzed reactions. Theoretically, the reaction rates could be increased by using higher concentrations of the bioorthogonal handles, but owing to constraints in nuclear medicine and *in vivo* applications solely alternative reaction pairs could ameliorate the situation.

To overcome all these obstacles, the groups of Fox and Weissleder described independently the inverse electron-demand Diels-Alder (IEDDA) reaction between 1,2,4,5-tetrazines and strained alkenes (including cyclopropene, norbornene etc. and especially *trans*-cyclooctenes (TCOs)).[7,8] These ligations show unprecedented second order rates (up to 10^6 M^{-1} s^{-1} for highly strained TCOs with bis-aryl tetrazines in water) representing a cornerstone in the history of bioorthogonal reactions.[9] In this irreversible [4+2] cycloaddition between 1,2,4,5-tetrazines and *trans*-cyclooctenes (TCO) an intermediate is formed that spontaneously rearranges by release of N_2 in a retro-Diels-Alder cycloaddition to a 4,5-dihydropyridazine (which may further tautomerize and finally aromatize) (Fig. 2d).[10] The expulsion of N_2 and the relief in ring strain are the driving forces of the reaction entailing its irreversibility.
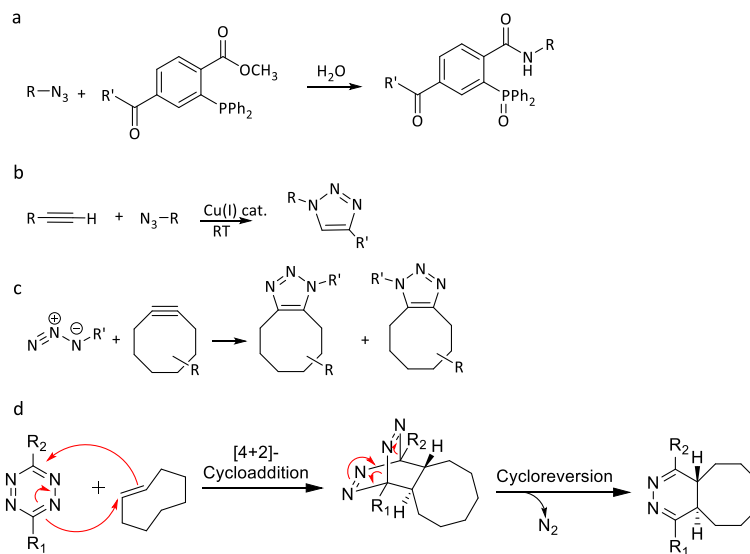
Figure 2: a) Staudinger ligation; b) CuAAC; c) SPAAC; d) Tetrazine ligation (with mechanism).

In contrast to the classic Diels-Alder reaction, one with inverse electron demand occurs between an electron-deficient diene and an electron-rich dienophile. For instance, conjugated dienes with heteroatoms like N (e.g. tetrazines) have due to their electronegativity a favorable lower lying LUMO. Principally, electron-withdrawing groups in the diene will lower the energy of its LUMO, while the addition of electron- donating groups in the dienophile implies a rise in energy of the HOMO (Fig. 3). Thus, the interaction between HOMO of the dienophile and the LUMO of the diene results in a smaller energy gap, a better overlap of orbitals and by implication in higher reaction rates.
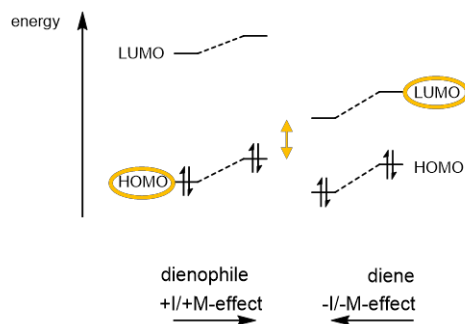

Figure 3: Schematic energy diagram to illustrate substituent effects of IEDDA

1.3 The Bioorthogonal Toolkit

In the field of bioorthogonal chemistry, scientists especially focused on developing bioorthogonal ligation reactions (or "bond formation" reactions). Compared to the rich methodology of organic chemistry (eg. substitutions; additions; eliminations; rearrangements; oxidations and reductions; condensations, metal catalysed coupling reactions (e.g. Suzuki coupling, Sonogashira coupling, Metatheses or CH activations) and combinations of the preceding, only one type - bioorthogonal addition - has been explored for bioorthogonal applications (Fig. 4).
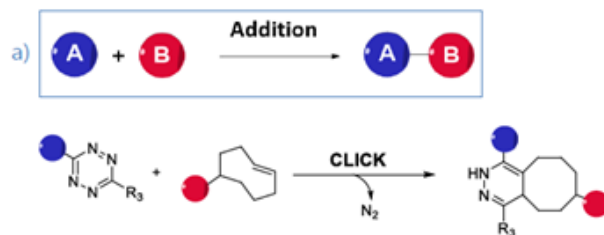
Figure 4: Bioorthogonal Ligation

More recently, a second class of Bioorthogonal Reactions, namely Bioorthogonal Eliminations has rapidly emerged. Robillard and co-workers concentrated on the IEDDA reaction designing an efficient elimination system by choosing a carbamate-functionalized TCO with a tetrazine (Fig. 5).[13] This so called "click to release" reaction has already found a variety of applications such as the efficient and fast activation of rTCO masked proteins[14] (rTCO = release TCO) and a novel prodrug activation method (e.g. antibody drug conjugate release).[15,16]
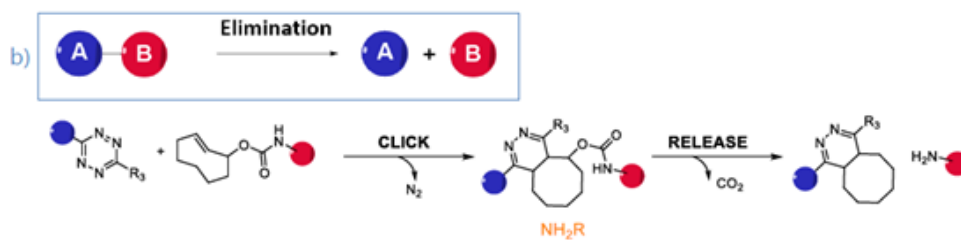

Figure 5: Bioorthogonal Elimination („click to release")

The starting point of the elimination step is the intermediate of the click reaction (i.e. dihydropyridazine). Thus, to trigger the release by deprotonation the leaving group has to be introduced in one of the allylic positions of the TCO (Fig. 6).
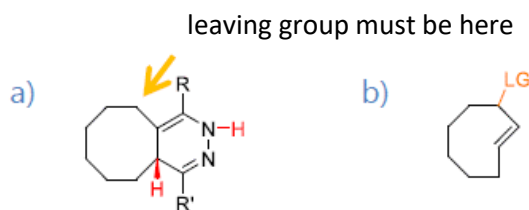
Figure 6: a) 1,4-Dihydropyridazine (intermediate) b) release TCO with leaving group (LG) in allylic position

Finally, the release will be solely induced by the preceding click avoiding any arbitrary losses of the leaving group. The mechanism of the reaction encompasses two steps, an addition and a subsequent elimination.[15] In the first step the already explained cycloaddition leads to a 4,5-dihydropyridazine followed by tautomerization to a 1,4-dihydropyridazine. The latter undergoes a deprotonation and a concomitant release of CO_2 providing the leaving group as a free amine (Fig. 7). The remaining pyridazine subsequently forms the more favorable aromatic pyridazine. However, aromaticity is not the driving force of the elimination reaction because the release of the free amine is much faster than the aromatization process.[15]

Figure 7: Mechanism of the elimination process adapted from Versteegen et al.[11]

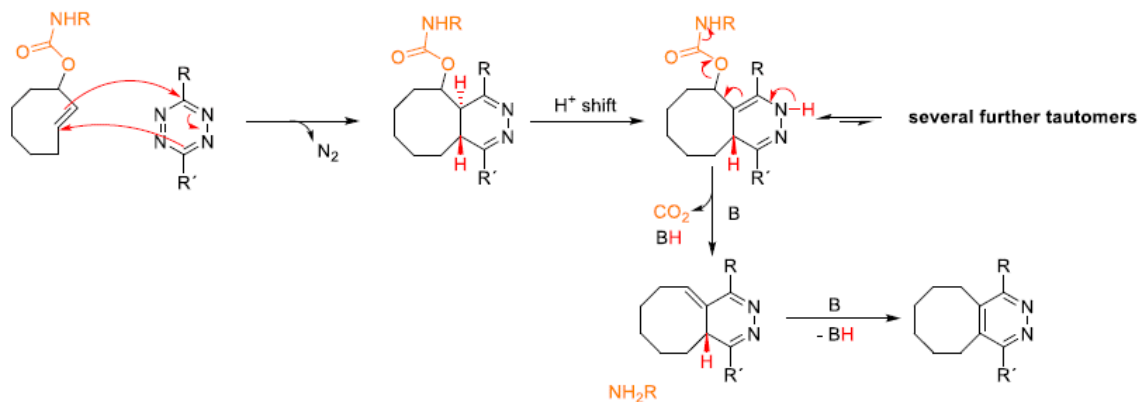Chen and co-workers have demonstrated based on a coumarin fluorogenic assay that both the click and the release rates are dependent on the substituents of the tetrazine.[12] The probably greater influence on the click rate stems from the type of TCO. Here, the most important role plays the ring strain. Therefore highly strained TCOs with enhanced click rates are already designed.[9] But so far, there are no TCOs, specially designed to accelerate the elimination process (release). One major aim of this project is to design new rTCOs with higher release rates (2nd generation rTCOs, Fig. 8). As mentioned above, elimination of the leaving group and formation of the pyridazine species is the rate-depending step. So, favouring elimination by installing a conjugated system and forcing the double bond to the proper position might be a promising strategy. This can be done by fusing an aromatic system (e.g. benzene, pyrrole, thienophene) to the TCO scaffold.
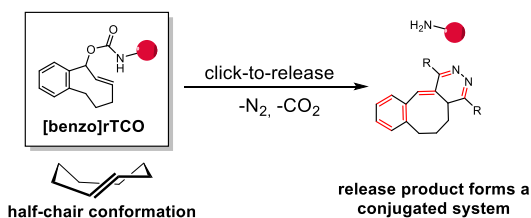

Figure 8: benzo[r]TCOs for faster release by installing a conjugated system to the TCO scaffold

Additionally the rTCO is forced into the energetically less favored half-chair conformation by fusing a benzene ring to the TCO scaffold to obtain a novel [benzo]rTCO (Fig. 8). The release product, besides the released amine, is a pyridazine moiety with a fully conjugated system, which is supposed to encourage the release step (Fig. 8).

1.4 Dienophiles

It is important to underline that internal olefins (i.e. unstrained) exhibit negligible rates with tetrazines meeting the requirement for bioorthogonal reactions because internal *cis*-alkenes are ubiquitous in nature (e.g. in fatty acids of phospholipids being part of the cell membrane). Only the introduction of ring strain does sufficiently destabilize this unsaturated functionality (decreasing its free activation enthalpy) to enable an IEDDA reaction in a reasonable time. As a result, either the ring size must be small enough to introduce strain in a *cis*-double bond or a *trans*-configuration must be selected. The smallest *trans*-cycloalkene known to date (i.e. stable at r.t.) is the *trans*-cyclooctene (TCO). It is less stable than its *cis*-

isomer arising from the twisted double bond (2p-orbitals make an angle of 44°). This increase in energy and hence drop of activation enthalpy implies a difference between the second order rate constants of the *cis*- and *trans*-isomer in 6 orders of magnitude for an IEDDA reaction (cis-cyclooctene: k_2 = 0.03 $M^{-1}s^{-1}$; *trans*-cyclooctene: k_2 = 12 700 $M^{-1}s^{-1}$).[10]

Classic *trans*-cyclooctene's most stable structure is a "crown" conformer having a chiral plane (Fig. 9 a). Similarly to the chair conformation of cyclohexane, the hydrogen atoms alternate in this structure in equatorial and axial positions. In contrast to six membered rings, the chair conformation is higher in energy (Fig. 8 a) at eight membered rings. To deal with the challenge of further acceleration, Fox and co-workers developed a TCO (i.e. bicyclo[6.1.0]non-4-ene; abbreviated as sTCO) forcing it into the less favored half-chair conformation by fusing a cyclopropane *cis* to the *trans*-cyclooctene resulting in the fastest reported reaction to date (k_2 = 3 300 000 $M^{-1}s^{-1}$ in water with 3,6-dipyridyltetrazine).[13] Figure 9 b presents the changes in energy of the reactants as a consequence of their structure (under the assumption that the energies of the transition states are similar). This strategy tipped the scales too much in favour of Diels-Alder reactivity having the difficulty of only moderate stabilities and of a strong hydrophobic character. Six years later, the same group came up, guided by computational considerations, with a new TCO overcoming the restrictions of the latter by annealing a dioxolane entity *cis* to the TCO (i.e. d-TCO), they achieved on the one side also a strained half-chair conformation but on the other side a compensating stabilization due to the –I-effectof oxygen. As a result, they created a highly reactive TCO (k_2 = 366 000 $M^{-1}s^{-1}$ in water with 3,6-dipyridyltetrazine) displaying at the same time a high stability and water solubility (imparted by two oxygen atoms of the dioxolane moiety). In contrast to the synthesis of azide and alkyne precursors, the production of TCO and tetrazine derivatives is often a laborious procedure. However, why is it worth to accept this inconveniences?
A glance at the comparison of the reaction rates speaks volumes (Staudinger Ligation: k_2 ~10^{-3} $M^{-1}s^{-1}$, Cu-free click chemistry: k_2 ~1 $M^{-1}s^{-1}$; tetrazine ligations k_2 ~10^6 $M^{-1}s^{-1}$).[3]
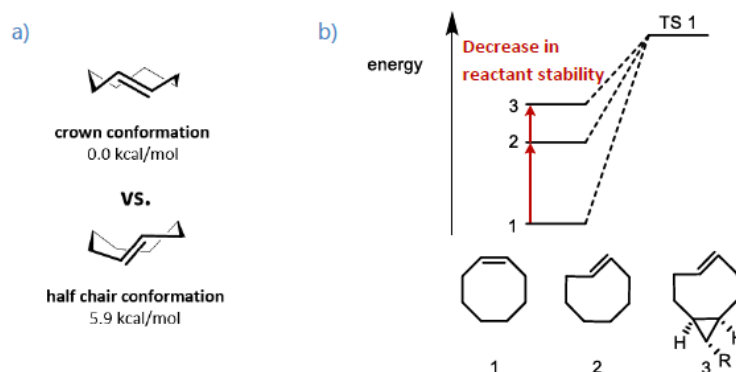
Figure 9: a) Two conformations of TCO. b) Schematic illustration of energy changes cis-Cycloocten (1), trans-Cycloocten (2) and sTCO (3); TS...transition state).

1.5 Photoisomerization of *trans*-cyclooctenes (TCOs)

The initially cumbersome multistep procedures for the inversion of olefins posed a problem in the synthesis of *trans*-cyclooctenes (TCOs). To deal with this problem, Fox and co-workers developed a direct strategy of TCO synthesis enabling the simple access to a myriad of functionalized derivatives.[14]
The underlying principle is the irradiation of *cis*-cyclooctenes with UV-C light (254 nm) and its equilibration between *cis*- and *trans*-isomer mediated by a singlet sensitizer (aromatic ester; e.g. methyl benzoate). Only the presence of the sensitizer allows the formation of the *trans*-isomer by interaction between the

excited singlet state of the sensitizer and the ground state of the cyclooctene isomers via an exiplex (double bond twisted by 90°) and subsequent decay. The *trans*-isomer can form in contrast to the *cis*-isomer a stable complex with silver cations (equilibrium constants for complex formation K_f between *cis*-cyclooctene, *trans*-cyclooctene and silver nitrate in ethylene glycol at 40 °C are 14.4 and >1000 L/mol, respectively; presumably the relief of ring strain involved enables a twisting of the double bond). To exploit this advantageous difference, our group developed a continuous photo-isomerization method, where the mixture of isomers is circulated through a cartridge filled with $AgNO_3$ impregnated silica trapping only the desired *trans*-isomer. Hence, the TCO is removed from the equilibrium, whereas the *cis*-isomer is flushed through the photoreactor again and a new reaction cycle can start. Lastly, after "complete" retention, the product is eluted by mixing the Ag^+ impregnated silica with NH_4OH. The stronger complex with ammonia (i.e. $[Ag(NH_3)_2]^+$) entails the release of the TCO. Figure 10 summarized the basis of this process.
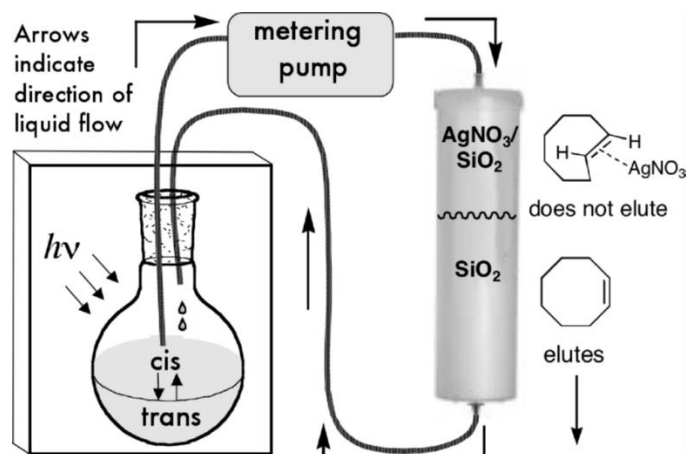
Figure 10: Principle of the photoisomerization

1.6 Dienophiles

The reaction rate constants of tetrazine ligations can be tuned in a range of several orders of magnitude by changing the electronic properties of the 1,2,4,5 tetrazine (Tz) moiety by varying the substituents in 3- and 6-position. In general, electron-withdrawing substituents increase, while electron-donating groups decrease Tz reactivity.[15] Tetrazines bearing an amino group are useful due to straight-forward conjugation to target molecules or further modification. An overview of selected amino-functionalized Tz and respective second order rate constants for the reaction with TCO (**1**) is shown in Figure 11.[16]
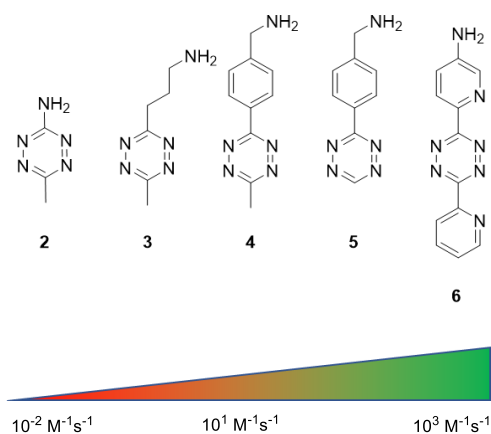
Figure 11: Overview of various tetrazines used in IEDDA ligations and respective second order rate constants for the reaction with TCO (room temperature, aqueous conditions).[17]

Aminotetrazine **2** exhibits low reactivity caused by the electron-donating effect of the NH_2 group directly attached to the Tz moiety. Dialkyltetrazine **3** shows only moderate reactivity due to the donating effect of the alkyl substituents,[18] while aryl/alkyl-substituted tetrazines such as **4** are slightly more reactive.[18,19] Monosubstituted tetrazines (H-tetrazines, H-Tz) such as **5** show high reaction rates (because of less steric hindrance)[20] similar to tetrazines bearing electron-withdrawing heteroaryl substituents such as pyridyl or pyrimidyl moieties (e.g. Tz **6**).[19] However, the applicability of highly reactive tetrazines is often limited due to low stability in biological media.[21] The choice of too strong electron-withdrawing substituents on the tetrazine might extremely accelerate the ligation reaction at the expense of a low water stability, thus, the structure loses its bioorthogonal character. Consequently, depending on the application, it is important to make always a compromise between the two opposing factors.

The first 1,2,4,5-tetrazines have already been reported at the end of the 19th century by Adolf Pinner and were prepared starting from iminoester hydrochlorides ('Pinner salts') and hydrazine forming an amidrazone as intermediate that reacts with excess hydrazine affording a dihydrotetrazine, which is finally oxidized to obtain 1,2,4,5-tetrazines (Figure 12 a).[22] In recent years, tetrazines have most commonly been synthesized by condensation of two nitriles with hydrazine followed by oxidation (Figure 12 b).[18,23] However, the preparation of alkyl-substituted Tz applying this method often results in low yields. A major improvement was achieved by Devaraj and co-workers by using Lewis acids for the activation of nitriles leading to significantly increased reaction yields.[18] A wide variety of aryl- and alkyl substituted tetrazines are accessible using this approach. A remaining drawback of the Lewis acid mediated tetrazine synthesis is the statistical mixture often obtained when using different nitriles to prepare unequally substituted tetrazines.[24] Alternatively, tetrazines can be synthesized using nucleophilic aromatic substitution using precursors mono- or bis-functionalized with 3,5-dimethylpyrazol or chlorine (Figure 12 c).[25] In general, these methods afford tetrazines with decreased or even very low reactivity. Already in the 1960s, Takimoto and co-workers presented a robust and straightforward synthesis for the production of unsymmetrical 3-aminotetrazines.[26] Therein, 3-azido-1,2,4-triazole-4-amines are thermally decomposed affording 3-aminotetrazines in good yields (Figure 12 d).
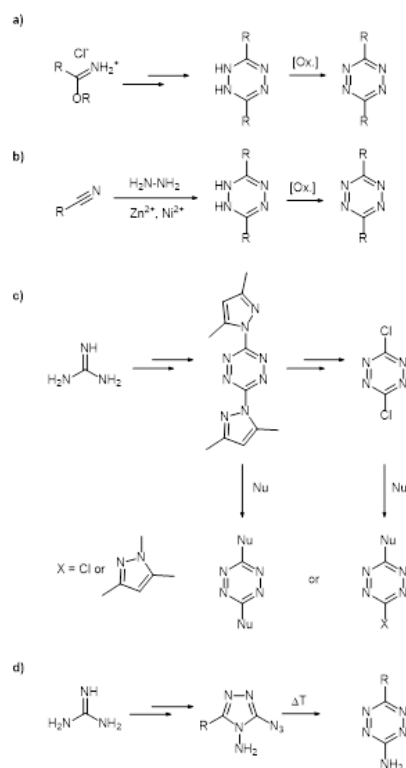
Figure 12: Methods for the preparation of 1,2,4,5-tetrazines. a) First tetrazine synthesis by A. Pinner; b) Lewis acid mediated Tz synthesis; c) 3,5-dimethylpyrazol-1-yl- or chloro-tetrazines and subsequent nucleophilic aromatic substitution; d) Synthesis of unsymmetrical aminotetrazines by thermolytic decomposition of 3-azido-1,2,4-triazole amines. Ox. = oxidation; Nu = nucleophile.

2 Results & Discussion

The 'click to release' reaction is used to combine two different targeting strategies achieving double-targeted prodrug activation inside tumor cells. Therefore, we designed a C_{16}-TCO-drug-conjugate encapsulated in nanoparticles (nano-prodrug, Fig. 13) that can be activated by bioorthogonal cleavage upon reaction with the activator (tetrazine-ligand conjugate, Fig. 13).

- Nano prodrug: nanoparticles are targeting to malignant tissues due to the EPR effect. The EPR-effect describes the enhanced permeation and retention of nanoparticles in malignant tissue because of the abnormal physiology and structure of tumor cells. The used C_{16} anchor ensures 100% encapsulation of the prodrug in the PLGA-PEG nanoparticles

- Activator: The tetrazine-ligand conjugate binds specific to proteins which are overexpressed on tumor cells. In this study the ligand ACUPA is used, which targets the Prostate-specific membrane-antigen (PSMA). PSMA is overexpressed in prostate cancer cells.
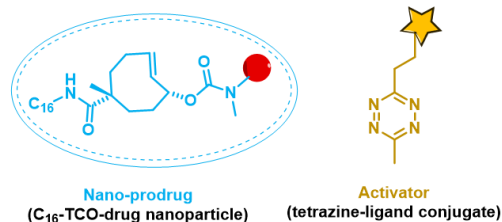
Figure 13: Structures of the nano prodrug and the activator

After both are internalized into tumor cell, the prodrug is activated by the bioorthogonal 'click to release' reaction (Fig. 14 a). Different distribution profiles of both compounds are utilized to achieve therapeutic prodrug activation only inside target cells (Fig. 14 b). We hypothesize that problems related to nonspecific distribution and high 'off-target' toxicity of each single compound can be circumvented by using this double targeting approach.
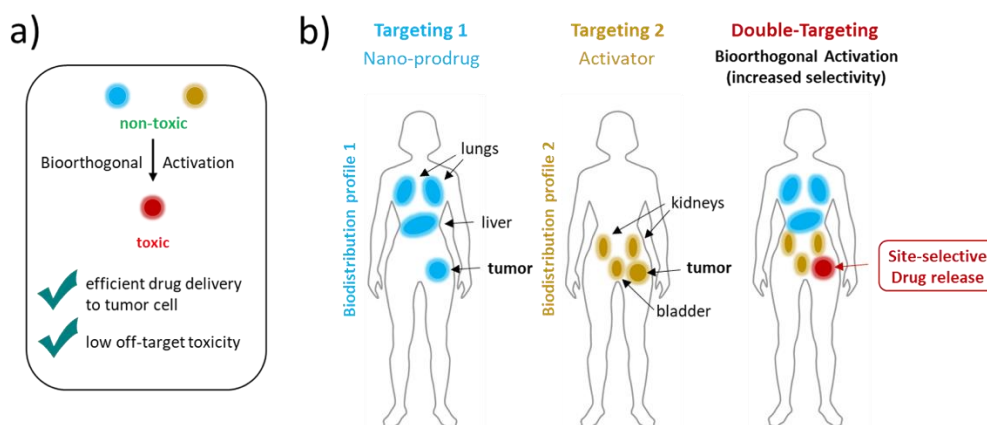
Figure 14: a) Bioorthogonal prodrug activation by the 'click to release' reaction; 3b) Principle of the double targeting approach

2.1 Synthesis

First, the C_{16}-TCO-drug conjugate and the activator had to be synthesized and characterized (NMR, HRMS). The needed building blocks (TCO, 1,2,4,5-tetrazine, ACUPA) were synthesized in Vienna and in the chemistry lab of my hosting institution, the Center for Systems Biology, Massachusetts General Hospital/Harvard Medical School (CSB, MGH/HMS) in Boston.

2.1.1 C_{16}-TCO-drug

First, a bicfunctional TCO was needed to obtain the desired C_{16}-TCO-drug conjugate. TCO must be linked at one handle with the C_{16} anchor, on the release position the TCO is modified with the drug MMAE. This important building block was made according to *Rossin et al:* [27]

A suitable synthesis route should afford facile isolation of diastereoisomers with the conjugation handle on the TCO in either the equatorial or the axial position and with an allylic hydroxyl in the axial position, as the equatorial hydroxyl-derived carbamate was previously shown to be 156-fold less reactive,[28] due to steric hindrance and, possibly, electronic effects.[28] In addition, it should allow subsequent orthogonal

manipulation of the conjugation handle and the hydroxyl group. A route was designed centering on the iodolactonization of 4-cyclooctene-1-carboxylic acid **10** followed by hydrogen iodide elimination and lactone hydrolysis to stereoselectively install the hydroxyl in the allylic position. A methyl group was introduced near the carboxylic acid of **10**, affording **11**, to prevent epimerization during lactone hydrolysis and to enable regioselective conjugation of TCO with MMAE (Figure 15).
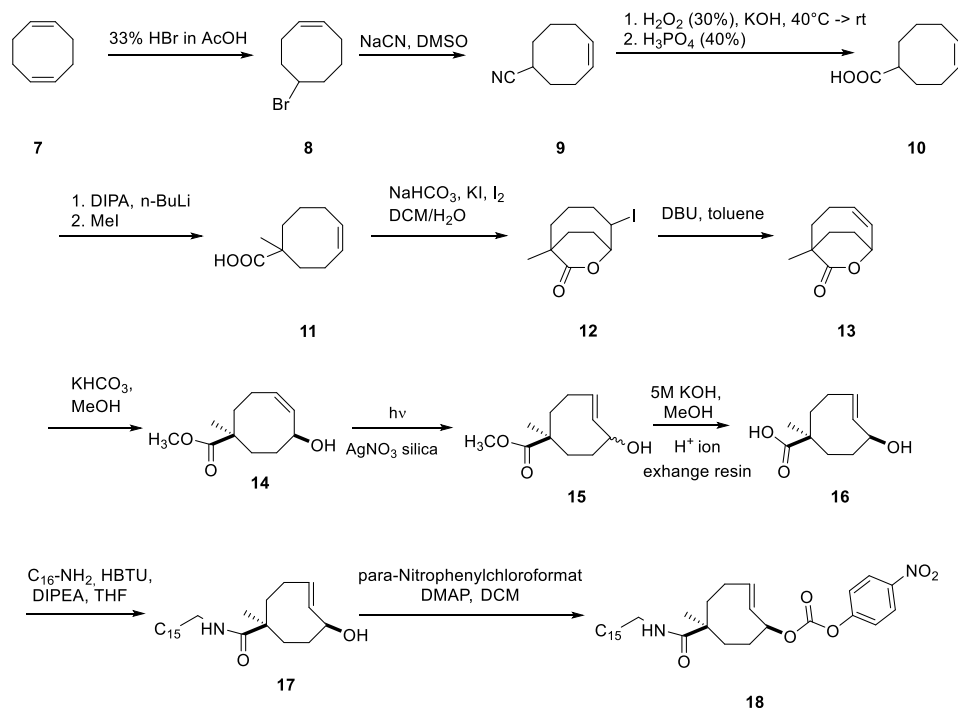

Figure 15: Multistep-synthesis towards C_{16}-TCO-PNP ester **18**

Compound **7** was prepared via an electrophilic addition of hydrobromic acid with subsequent straightforward distillation removing the remaining reactant and the dibromo cyclooctane side product. Nucleophilic substitution of the bromide by cyanide gave the nitrile **8**. Predominantly, dimethyl sulfoxide is used as solvent for this reaction in literature, albeit the lethal combination of the highly toxic salt NaCN and the enormous carrier ability of DMSO through the skin. This may be attributed to its good ability of solvating cations (with the partial negative charge on the surface of the molecule) and a poor ability to solvate anions (partial charge of DMSO on the "inside" is less accessible) hence providing a stronger nucleophile (due to the rather "naked" presence of CN- in solution). Special precautions had to be taken particularly when extracting 2 L of this highly toxic mixture in water (wearing a whole body protective suit).

The third step encompasses the base-mediated hydrolysis of the nitrile being accelerated with addition of hydrogen peroxide. The underlying principle is the presence of hydroperoxide ions (in equilibrium with hydroxide, water and hydrogen peroxide) being stronger nucleophiles than hydroxide ions due to the α-effect (overlap of orbitals containing the electron pairs of the adjacent oxygen atoms results in an increase of HOMO energy). Usually the mentioned mixture provides the amide via a partial hydrolysis. However, under the harsh conditions applied in the procedure (refluxing in 30 % NaOH) a total hydrolysis takes place being indicated by the release of ammonia. The acidification in the second step ensures the completion of the hydrolysis and protonates the carboxylate for the following work up affording 40 g of compound **10**. In spite of an additional step compared to other routes and a risky work up procedure, the latter

reaction sequence should be favored for gram scale preparations due to a 2.5-fold overall yield, much cheaper reactants and a straightforward performance.

Next, compound **10** was treated with two equivalents of the strong non-nucleophilic base LDA to deprotonate both the carboxylic acid and its α-H atom giving an enolate dianion. Since the low acidity of this α-H and the relative stability of the dianion (compared to an α-ester) harsh temperature jumps (between -50 and +50 °C) had to be performed. Subsequent methylation with the strong electrophile methyl iodide yielded **11**.

Iodolactonization of **11** was conducted in a two-phase system of dichloromethane and $NaHCO_3$ in water. Apart from iodine as reactant, potassium iodide was used to improve its water solubility by forming the triiodide ion. Initial deprotonation of **11** by hydrogencarbonate results in its transfer to the aqueous phase where positive iodine (from I_3) is added to the double bond. The addition may occur on both sides of the molecular plane but the subsequent ring-closing (preferring a six membered to a seven membered ring) by a backside attack of the carboxylate is essentially only possible from one side affording one isomer of **12**. After the intermolecular substitution reaction, the molecule loses its charge and hence is removed from the reaction phase by the transfer back to the organic layer. This shows the efficiency of applying a two phase system for iodolactonization.

The previous two steps are of particular significance to minimize the number of diastereomers resulting from photoisomerization because the iodolactonization provides a strategy to place both upcoming functionalities in a fixed stereoselective relationship (here *cis*) and the α-methyl group avoids epimerization upon hydrolysis of **14**. Elimination of hydrogen iodide by the non-nucleophilic base DBU gave **13** in a yield of 83%. An alternative elimination would be disfavored by an enormous ring strain (Bredt's rule). The following base-mediated ring-opening of the enelactone, finally created the two functionalities required for conjugation *cis* to each other in a single diastereomer **14**. A detailed investigation of a similar reaction in literature disclosed the reason for choosing MeOH with $KHCO_3$ instead of the intuitive methanolate.[29] They reported that the ring-opening with methanolate leads to an undesired ether and acid combination rather than to a hydroxyl and an ester functionality. Photoisomerization according the above described procedure gave the TCO **15** as a mixture of two conceivable diastereomers, with the hydroxyl group in axial position (corresponding to the ester functionality in equatorial position) and the diastereomer with the hydroxyl group in equatorial position (corresponding to the ester in axial position). The separation of this mixture could be achieved by flash column chromatography. The desired diastereomer with the hydroxyl group in the axial position is less polar and elutes first by applying a mobile phase of hexanes/dieethylether 20-40%. The methyl ester was hydrolysed with 5M KOH in MeOH, after complete conversion (2h) reaction was neutralized with Amberlite IR 120 H^+ ion exchange resin. Crude was concentrated under *vacuo*. A 50 mM solution of 1.1 eq. C_{16}-NH_2 in THF was added to a mixture of **16**, 1.1 eq. HBTU and 10 eq. DIPEA in DMSO. After 30 min stirring, reaction mixture was loaded onto a C4 $50\mu m$ column and **17** was obtained by applying a gradient of Water/Acetonitrile 5-99% as a beige solid.

For further modification, the allylic alcohol must get activated. This was achieved by stirring **17** in DCM and cooling down the resulting solution to 0°C with an ice bath. 4 eq. 4-Dimethylaminopyridine (DMAP) and 2 eq. 4-para-Nitrophenylchloroformiate (PNP-chloroformiate) were added and the mixture was stirred at room temperature overnight. Crude was concentrated under reduced pressure and **18** was received by conducting normal phase flash column chromatography (silica, hexanes/dieethylether 10-40%) as white-off solid.

The further modification (Fig. 16) was connecting **18** to the antimitotic agent Monomethyl auristatin E (MMAE). This was done by dissolving **18** in DMF and adding 1-Hydroxybenzotriazole (HOBt), Diisopropylethylamin (DIPEA) and MMAE. After 30 min stirring at room temperature, the mixture was loaded onto a C4 flash column and eluted by an gradient of Water/Acetonitrile 5-99%. **19** was yielded as coloress solid (see Fig. 16).
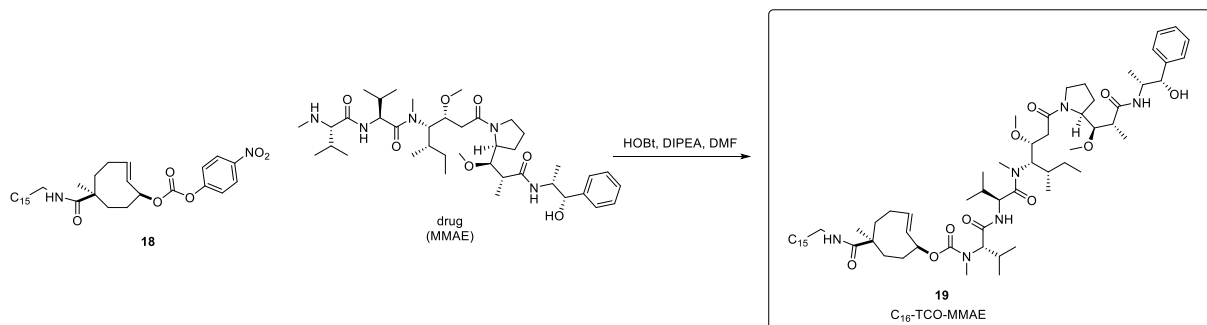

Figure 16: Synthesis of C_{16}-TCO-MMAE

The chosen drug Monomethyl auristatin E (MMAE) is an antimitotic agent, which inhibits cell division by blocking the polymerisation of tubulin. The C_{16} anchor is necessary for the next step, the encapsulation of the C_{16}-TCO-drug conjugate into PLGA-PEG nanoparticles.

2.1.2 ACUPA

ACUPA (2-(3-((S)-5-amino-1-carboxypentyl)ureido)pentanedioic acid) is used as a target ligand which targets Prostate-specific membrane-antigen (PSMA). The level of expressed PSMA is increased in prostate cancer cells (PCa) than in normal prostate issue. The genomics researches and pathological analysis have proved that PSMA is one of the most enhanced expression proteins in PCa, and the PSMA expression level shows a positive correlation with the risk of tumor progress or metastasis.[30] In the last years, several strategies have been developed to enable targeting capacity for PCa in PSMA targeted prodrugs or nanomedicines, such as peptides, RNA aptamers and monoclonal antibodies (mAb). 2-[3-(1,3-Dicarboxypropyl)ureido]pentanedioic acid (DUPA) is one of the highest-affinity small molecular ligands of PSMA. After binding to PSMA, DUPA can be immediately endocytosed into clathrin-coated pits, and PSMA can release DUPA into cytoplasm and then return to the cell membrane. It was shown, that DUPA-linked cytotoxins can efficiently inhibit tumor proliferation both *in vitro* and *in vivo* with moderate to good specificity. As a chemical mimic of DUPA, 2-(3-((S)-5-amino-1-carboxypentyl)ureido)pentanedioic acid (ACUPA) also shows satisfactory targeted efficiency at the protein, cell and whole animal levels.[31]

Synthesis of the tert. butyl ester protected ACUPA building block was conducted according to *Zhang et al* (Fig. 17)*:*[32]
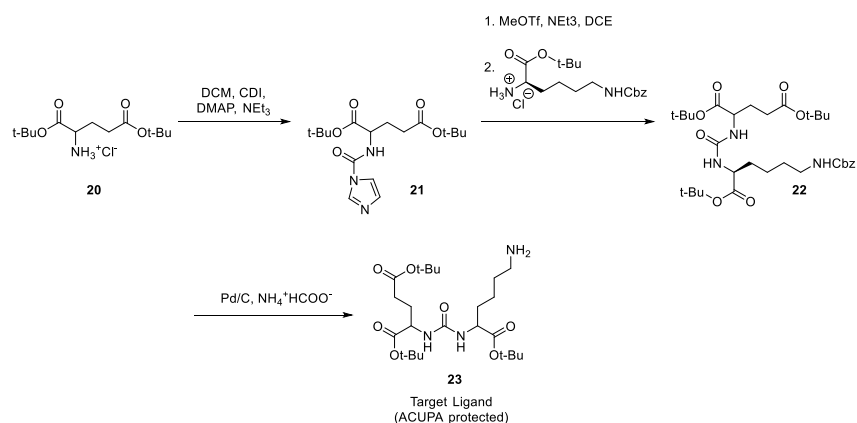
Figure 17: Synthesis of the tert. butyl ester protected ACUPA building block

(S)-2-[(Imidazole-1-carbonyl)amino]pentanedioic Acid Di-tertbutylEster (**21**):
To a suspension of L-di-tert-butyl glutamatehydrochloride (15.0 g, 51 mmol) in DCM (150 mL) cooled to 0°C was added TEA (18 mL) and DMAP (250 mg). After the mixture was stirred for 5 min, CDI (9.0 g, 56 mmol) was added and the mixture was stirred overnight with warming to room temperature.The mixture was diluted with DCM (150 mL) and washed with saturated sodium bicarbonate (60 mL), water (2 × 100 mL), and brine (100 mL). The organic layer was dried over sodium sulfate and concentrated to afford the crude product as a semisolid, which slowly solidified upon standing. The crude material was triturated with hexane/ethyl acetate to afford a white solid which was filtered, washed with hexane (100 mL), and dried to afford the desired product **21** (15.9 g, 45 mmol, 88%)

(S)-2-[3((S)-(5-Benzyloxycarbonylamino)-1-tert-butoxycarbonylpentylureido]pentanedioic Acid Di-tert-butyl Ester (**22**).
To a solution of **21** (1 g, 2.82 mmol) in DCE (10 mL) at 0 °C was added Methyltrifluormethylsulfonat (Methyltriflat, MeOTf, 0.47 g, 2.85 mmol) and trieethylamine (0.57 g, 5.65mmol). After the solution was stirred for 30 min, Cbz-Lys-Ot-Bu (1.06 g, 2.82 mmol) was added in one portion and allowed to stir for 1 h at 40 °C. The mixture was concentrated to dryness and purified by column chromatography (SiO$_2$) to afford the desired product as a white solid

2-[3-(5-Amino-1-tert-butoxycarbonylpentyl)ureido]pentanedioic Acid Di-tert-butyl Ester (**23**).
To a solution of (S)-2-[3-(5-benzyloxycarbonylamino-1-tert-butoxycarbonylpentyl)ureido]-pentanedioic acid di-tert-butyl ester (**22**) (630 mg, 1.0 mmol) in ethanol (20 mL) was added ammonium formate (630 mg, 10 eqv) followed by 10% Pd-C, and the suspension was allowed to stand with occasional agitation overnight until complete. The mixture was filtered through Celite and concentrated to afford the desired product (479 mg, 0.98 mmol, 98%) as a waxy solid.

2.1.3 ACUPA-MPA

1,2,4,5 tetrazine-methyl propionic acid (MPA) was the next building block we synthesized. The common way to synthesize 1,2,4,5 tetrazines is with hydrazine and lewis acids like Zn(OTf)$_2$. To a 10 mL microwave reaction tube equipped with a stir bar, 0.6 eq of Zn(OTf)$_2$, 10 eq. of acetonitrile, 10 eq. of anhydrous hydrazine and 1 eq. of propionic acid was added. The vessel was sealed and the mixture was stirred in an oil bath at 60°C for 24 hours. After reaction, the seal was removed and the reaction solution was cooled to room temperature. Sodium nitrite (5 eq.) in 10 mL of water was slowly added to the solution and

followed by slow addition of 1M HCl during which the solution turned bright red in color and gas evolved. Addition of 1M HCl continued until gas evolution ceased and the pH value is 3. (Caution! This step generates a large amount of toxic nitrogen oxide gasses and should be performed in a well ventilated fume hood). The mixture was extracted continuously with ethylacetate overnight and the organic phase was dried over sodium sulfate. The solvent was removed using rotary evaporation and the residue purified using silica column chromatography (dicholoromethane/ethylacetate 3:2 +0.1% acetic acid).
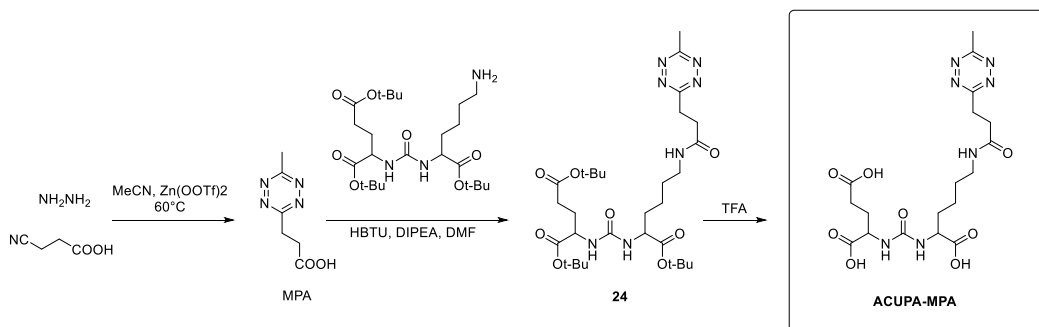

Figure 18: Synthesis of ACUPA-MPA

The next step was linking the target ligand ACUPA (tert. butyl ester protected) with MPA. Therefore, MPA was dissolved in DMF and DIPEA (4 eq.) and HBTU (1.1 eq.) was added. After 5 minutes ACUPA dissolved in DMF was added dropwise. The reaction mixture was stirred for 30 minutes and loaded onto a Biotage Snap Ultra 25 μm C18 column. **24** was yielded by applying a gradient of Water/Acetonitrile 5-95% +0.1% formic acid as white-off solid.

Final step was the deprotection of the three tert. butyl esters with trifluoroacetic acid (TFA). **24** was dissolved in trifluoroacetic acid and stirred overnight at room temperature. Next day, final product ACUPA-MPA was obtained after purification by prep HPLC (C18 Phenomenox Luna) with Water/Acetonitrile 2-30% + 0.1% formic acid (see Figure 18).

2.2 Nanoparticles

2.2.1 EPR-effect

The observation that nanoparticles accumulate preferentially to tumors was reported more than 30 years ago.[33] The tumor accumulation of therapeutic macromolecules was first witnessed for poly(Styrene-co-Maleic Acid)-NeoCarzinoStatin (SMANCS), a 16 kDa polymer conjugate that non-covalently binds albumin in the circulation to reach a molecular weight of around 80 kDa. The distribution of SMANCS to the tumor vicinity was observed in early preclinical development and led to further investigations.[33] Using labelled albumin and other proteins in addition to the polymer conjugate, they showed that proteins larger than 30 kDa favors to distribute to the tumor interstitium and remain there for prolonged periods of time.[33] This preferential distribution to the tumors was ascribed to the presence of fenestrations in the imperfect tumor blood vessels and to the poor lymphatic drainage in the tissue. The combination of these two phenomena was named as the **enhanced permeation** and **retention** effect (EPR). Since then, the EPR effect has become the thriving force for many scientists for the targeted delivery of anticancer drugs to tumors.

When a solid tumour reaches a certain size, the normal vasculature in its vicinity can not provide all the oxygen supply required for its further growth. As cells begin to die, they secrete growth factors that enhance the building of new blood vessels from the surrounding capillaries. This process, known as angiogenesis, promotes the fast creation of new, irregular blood vessels that present a discontinuous epithelium and lack the basal membrane of normal vascular structures. When blood components reach the abnormal, discontinuous vascular bed, the fenestrations offer little resistance to extravasation to the tumor interstitium. This indicates the enhanced permeation portion of the EPR effect. In normal tissues, the extracellular fluid is constantly drained to the lymphatic vessels. This allows the continuous draining and renewal of interstitial fluid and the recycling of extravasated solutes and colloids back to the circulation. In tumors, the lymphatic function does not work proper, resulting in minimal uptake of the interstitial fluid. As a result, the colloids cannot rely on convective forces to return to circulation. While molecules smaller than 4 nm can diffuse back to the blood circulation and be reabsorbed, the diffusion of macromolecules or nanoparticles (NPs) is hindered by their larger hydrodynamic radii. Therefore, nanoparticles that have reached the perivascular space can not cleared efficiently and thus accumulate in the tumor interstitium. This aspect represents the enhanced retention component of the EPR effect.[34]

2.2.2. Nanoencapsulation

A successful nanodelivery system should have a high drug-loading capacity, thereby reducing the quantity of matrix materials to the tissue. Targeted delivery can be actively or passively achieved. Active targeting requires the therapeutic agent to be achieved by conjugating the therapeutic agent or carrier system to a tissue or cell-specific ligand. Passive targeting is achieved by incorporating the therapeutic agent into a macromolecule or nanoparticle that passively reaches the target organ. Drugs encapsulated in nanoparticles or drugs coupled to macromolecules can passively target tumors through the EPR effect.

My supervisor at CSB/MGH/HMS, Dr. Miles Miller recently developed a new encapsulation method (Figure 19) with C_{16} drug conjugates, which showed an almost 100% encapsulation of the conjugate into PLGA-PEG nanoparticles.[35] The same encapsulation method was also used for the synthesis of the nano prodrug described above. PLGA-PEG nanoparticles were chosen, because they are already well established for targeted drug delivery systems and their behavior and biodistribution are well understood.
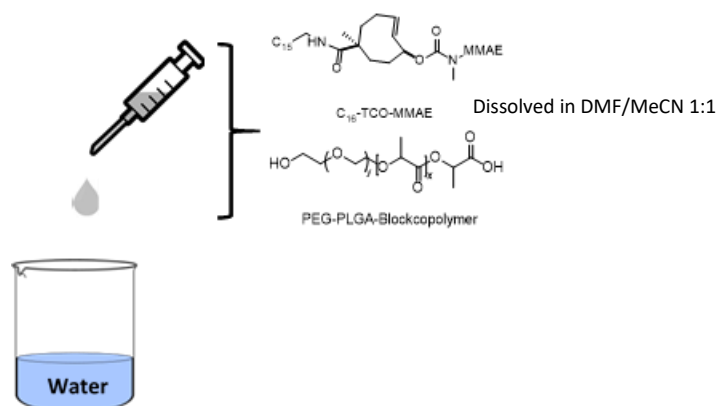

Figure 19: Principle of the synthesis of the PLGA-PEG nanoparticles

The nano prodrug was synthesized by nano-precipitation by first combining 1 mg of the synthesized C_{16} TCO drug conjugate, 5 mg PLGA 8.3kDa-PEG5.5kDa and 1 mg PLGA30-60kDa in a 212 µl mixture of 1:1

dimethylformamide (DMF) : acetonitrile (MeCN), then added drop-wise to 20 mL H_2O under stirring at r.t. for 4 h (Fig. 19), followed by filtering through a 0.45 μm cellulose acetate syringe filter and concentrated in 100 kDa molecular-weight-cutoff centrifugal filters spun at 3000 x g for 30 min. NP drug loadings were determined by HPLC/MS interpolation from a standard curve (R^2 >0.99) after 1:10 dilution in DMF. Size and zeta potential measurements were performed using dynamic light scattering.[36]

2.3 Tissue culturing

The two major advantages of tissue culture are the ability to control the physiochemical environment (pH, temperature, osmotic pressure, and O_2 and CO_2 tension), which must be controlled very precisely, and the physiological conditions, which have to be kept relatively constant. However, the physiological environment cannot always be defined where cell lines still require supplementation of the medium with serum or other poorly defined constituents. These supplements are prone to batch variation and contain undefined elements such as hormones and other stimulants and inhibitors. The identification of some of the essential components of serum, together with a better understanding of factors regulating cell proliferation, has made the replacement of serum with defined constituents feasible. The role of the extracellular matrix (ECM) is important, but similar to the use of serum—that is, the matrix is often necessary, but not always precisely defined. Prospects for defined ECM improve, however, as cloned matrix constituents become available.

2.3.1 Fluorescence microscopy

With the nano prodrug and the activator in our hand, we started first *in vitro* assays. First, appropriate cancer cell lines had to be selected. The selection was based on experiments with a fluorescence microscope. Fluorescence microscopy is a basic requirement in cell biology, molecular biology and biotechnology. Advancements over the past years has helped scientist to trace molecules in live cells and understand the basis of cell metabolism, exchange, mutation and toxicity. Substances used in fluorescence microscopy by virtue of its ability to fluorescence are called "fluorophores". Such substances are capable of being excited. This is so, because they can absorb energy from photons: The outermost orbital of this substances is important as it determines the fluorescence properties the excitation wavelength and emission wavelength. After excitation has passed, the molecule is capable of losing the absorbed energy by emission of fluorescence and return to the ground state by a mechanism called vibrational relaxation at which the electrons return back to the outermost orbital. The orbitals close to the nucleus has great electrical and low vibrational energy while the outermost orbitals have high vibrational but low electrical energy. Thus, the movement of electrons from the inner orbital to the outermost orbital involves energy conversion from electrical energy to vibrational force.[37]

Imaging experiments with a fluorescence microscope were conducted to see, whether ACUPA gets internalized into certain cell lines or not. Hence, several cell lines were incubated with a fluorescent ACUPA-dye conjugate. Exactly, a far-red dye called SiR (silicon rhodamine, Fig. 20 c) was used for this purpose. After we screened thoroughly, LNCaP and PC3 cells were chosen as cell models. LNCaP cells show a very high level of PSMA. LNCaP cells are androgen-sensitive human prostate adenocarcinoma cells, taken out from the left supraclavicular lymph node metastasis from a 50-year-old caucasian male in 1977.[38] They are adherent epithelial cells growing in aggregates and as single cells. One major obstacle for the most clinically relevant prostate cancer (PCa) research has been the lack of cell lines that closely mimic human disease progression. Two hallmarks of metastatic human prostate cancer include the shift of aggressive PCa from androgen-sensitivity to an Androgen Insensitive (AI) state, and the propensity of PCa to metastasize to bone. Although the generation of AI cell lines has been quite successful as demonstrated in the "classic" cell lines DU145 and PC3, the behavior of these cells in bone does not fully mimic clinical human disease. It is well established that human PCa bone metastasis form osteoblastic lesions rather than osteolytic lesions seen in other cancers like breast cancer. Similarly, PC-3 and DU145 cells form osteolytic tumors.[38]

The base medium for this cell line is RPMI 1640 medium. To make the complete growth medium, fetal bovine serum (FBS) was added to the base medium to a final concentration of 10%. T-75 flasks were used for subculturing. The subculturing procedure was as followed: First, old culture medium was removed and discarded and cells were washed with 10 mL PBS (phosphate buffered saline) to remove all traces of serum that contains trypsin inhibitor. Next, 2.0 to 3.0 mL of Trypsin-EDTA solution were added to flask and observe cells under an inverted microscope until cell layer is dispersed (usually within 5 to 15 minutes). To avoid clumping do not agitate the cells by hitting or shaking the flask while waiting for the cells to detach. Cells that are difficult to detach may be placed at 37°C to facilitate dispersal. Then, 6.0 to 8.0 mL of complete growth medium were added and cells aspirated by gently pipetting. Appropriate aliquots of the cell suspension were added to new culture vessels. Cultures were maintained at a cell concentration between 1×10^4 and 2×10^5 cells/cm^2 and at temperatures at 37°C. Cells were subcultivated with a ratio of 1:3 to 1:6.

In contrast to LNCaP, PC3 cells show a low expression level of the targeted protein PSMA. Thus, this cell line was chosen as negative control for further cell viability assays. PC3 cells are useful in investigating biomedicinal changes in advanced prostate cancer cells and in assessing their response to anticancer agents. The PC3 cell line was established in 1979 from bone metastasis of grade IV of prostate cancer in a 62-year-old Caucasian male.[39] These cells do not respond to androgens, glucocorticoids or fibroblast growth factors, but results suggest that the cells are influenced by epidermal growth factors. PC3 cells can be used to create subcutaneous tumor xenografts in mice to investigate the tumor environment and therapeutic drug functionality. PC3 cells have high metastatic potential compared to DU145 cells, which have a moderate metastatic potential, and to LNCaP cells, which have low metastatic potential. Comparisons of the protein expression of PC3, LNCaP, and other cells have shown that PC3 is characteristic of small cell neoendocrine carcinoma.[39]

The base medium for this cell line is F-12K Medium. To make the complete growth medium, fetal bovine serum (FBS) was added to the base medium to a final concentration of 10%. T-75 flasks were used for subculturing. The subculturing procedure was as followed: First, old culture medium was removed and discarded and cells were washed with 10 mL PBS (phosphate buffered saline) to remove all traces of serum that contains trypsin inhibitor. Next, 2.0 to 3.0 mL of Trypsin-EDTA solution were added to flask and observe cells under an inverted microscope until cell layer is dispersed (usually within 5 to 15 minutes).

To avoid clumping do not agitate the cells by hitting or shaking the flask while waiting for the cells to detach. Cells that are difficult to detach may be placed at 37°C to facilitate dispersal. Then, 6.0 to 8.0 mL of complete growth medium were added and cells aspirated by gently pipetting. Appropriate aliquots of the cell suspension were added to new culture vessels. Cultures were maintained at a cell concentration between 1×10^4 and 2×10^5 cells/cm^2 and at temperatures at 37°C. Cells were subcultivated with a ratio of 1:3 to 1:6.

Imaging experiments with a fluorescent ACUPA-dye conjugate (ACUPA-SiR, Fig. 20 c) revealed a 10-fold higher uptake of ACUPA into LNCaP (positive control) cell than into PC3 cells (negative control, Fig. 20 a and 20 b).
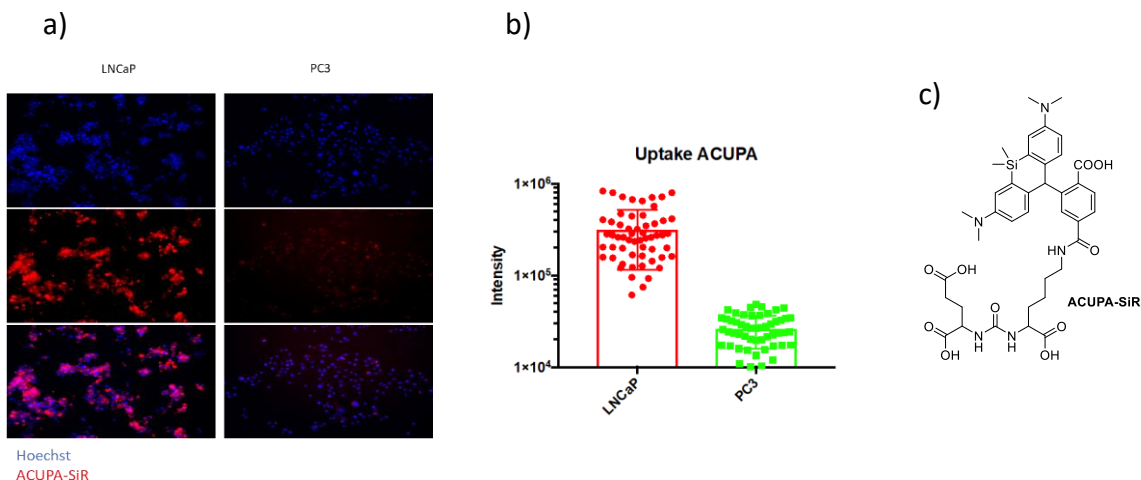

Figure 20: a) Imaging of LNCaP and PC3 cells with Hoechst (marks the nuclei) and fluorescent labelled target ligand (ACUPA-SiR). b) Imaging experiment shows that ACUPA uptake is 10-fold higher into LNCaP (PSMA pos.) than into PC3 cell (PSMA neg.) c) Structure of the used ligand-dye conjugate ACUPA-SiR

2.3.2 Cell Viability Assays

Based on these promising results, cytotoxicity assessments were conducted with LNCaP and PC3 cells. Different incubation times of the activator ACUPA-MPA and nano-prodrug were screened. Incubation of the activator for 1 hour followed by removing old media and adding the nano-prodrug exhibited best results.

Detailed procedure: 5000 cells per well were added to 96-well plates, cells were treated after overnight seeding with i) the nano-prodrug only; ii) MMAE itself; iii) activator ACUPA-Tz and the nanoprodrug simultaneously (co-incubation); iv) the activator ACUPA-Tz incubated for 1 hour followed by removing old media and adding the nano-prodrug. Cells viability was assessed after 72 h using PrestoBlue© reagent (Life Technologies) PrestoBlue Cell Viability Reagent is a ready-to-use reagent for rapidly evaluating the viability and proliferation of a wide range of cell types. PrestoBlue is quickly reduced by metabolically active cells, providing a quantitative measure of viability and cytotoxicity in as little as 10 minutes. Reagent was used following the manufacturer's protocol:[40]

- PrestoBlue Cell Viability Reagent is supplied as a 10X solution. Add PrestoBlue Reagent directly to cells in culture medium to obtain a 1X solution in cells + media suspension.

- Incubate ≥10 minutes at 37º C. Longer incubation times will increase sensitivity of detection. As we did cell assays, readings were taken at multiple time points to determine optimal performance. Top-read fluorescence was done with 20 min and 30 min incubation time. No significant difference was obtained.
- Read fluorescence or absorbance. Fluorescence is more sensitive than absorbance and is the detection method which was used.
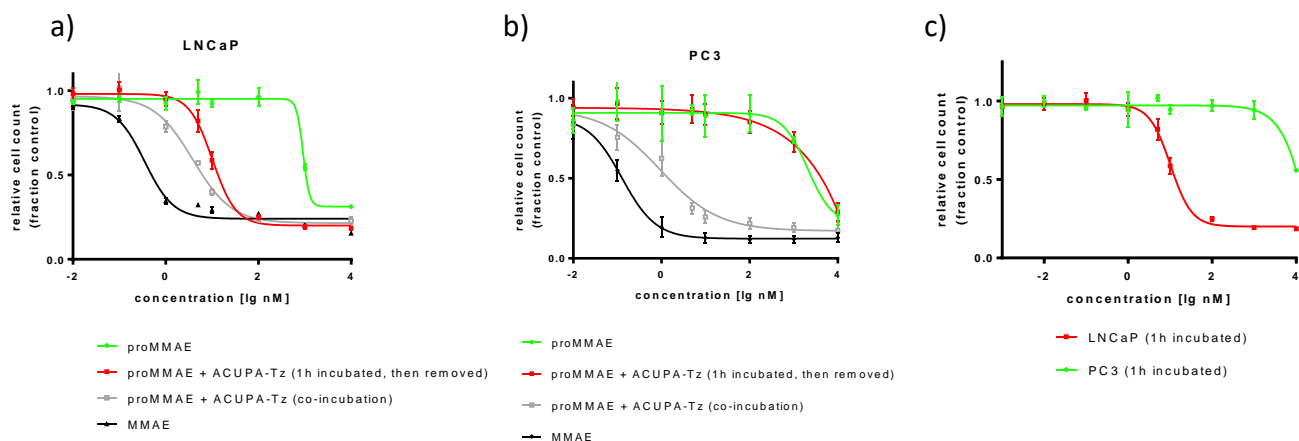

Figure 21: Results of the cell viability assay with a) LNCaP and b) PC3; ACUPA-Tz is also non-toxic in used concentrations (not shown here); 10 µM ACUPA-Tz was used for bioorthogonal activation; c) Comparison of LNCaP and PC3 results. Bioorthogonal activation is ~1000-fold increased in LNCaP cells.

These cell viability assays show an outstanding difference between PSMA-negative PC3 and PSMA-positive LNCaP cells (Fig. 21). Bioorthogonal nano-prodrug activation is around 1000-fold increased in LNCaP cells in comparison to PC3 cells. This means, that at a concentration of 50 nM of nano prodrug 50% of the LNCaP cells are killed by the activated prodrug (MMAE) and all PC3 cell are still viable. 50% of the PC3 cells are only dead at a very high concentration of 10 μM nano prodrug. Reason for this high IC$_{50}$ is, that no activator ACUPA-MPA got internalized into the PSMA negative PC3 cells.

3 Conclusion

These great results allow us to start first *in vivo* experiments in mice. Because there is no EPR-effect in 2D cultured cells, we expect even better results in mice, where EPR-effect should farther decrease 'off-target' toxicity and the double targeting approach can be fully effective. However, toxicity of the parent drug MMAE was not reached at the *in vitro* experiments. Even when activator and nano-prodrug were incubated at the same time (co-incubation), toxicity is around 100-fold less than toxicity of MMAE. Therefore, new tetrazines were currently designed to improve the yield of the 'click-to-release' reaction and to achieve a better biorthogonal activation.

During this research stay synthesis of needed compounds was finished, the nano prodrug was made, proper cell models were found by conducting imaging experiments and best conditions for cell viability assays were investigated and found. Luckily, results are very promising and *in vivo* experiments are under investigation. The huge progress of this project within the last 6 months would not have been possible

without the Marshall Plan scholarship. Because of the very interdisciplinary surrounding at my host institution (chemistry, cell biology, microscopy, bioengineering, nanosciences, etc), I learned many skills and techniques, which are beyond the typical skills of an organic chemist. In this year, I will transfer these skills to my home institution, the Institute of Applied Synthetic Chemistry at the Vienna University of Technology to improve there the know-how regarding microscopy, cell culturing etc.

I always wanted to stay a semester in the USA and because of the Marshall Plan scholarship this dream became possible. On the one hand, this internship helped to improve my English, on the other hand it certainly contributed to my personal development like learning a new culture and meeting new people. This stay abroad also served as an opportunity to establish new contacts within the scientific community and to build up an international scientific network. The Marshall Plan Scholarship was a great chance for me to obtain new theoretical knowledge and valuable practical skills. Receiving the Marshall Plan Scholarship allowed me to fulfill a great desire and may have an important contribution to my future career.

This fellowship broadened my scientific horizon in one of the world's leading research groups in this young and emerging field of chemical biology. Furthermore, we expect that this versatile double targeting approach enables many applications in targeted drug delivery systems and might pave the way for cancer therapies with less harmful side effects.

1. <u>References</u>

1. Sletten, E. M. & Bertozzi, C. R. Bioorthogonal Chemistry: Fishing for Selectivity in a Sea of Functionality. *Angew. Chemie Int. Ed.* **48,** 6974–6998 (2009).
2. Lin, F. L., Hoyt, H. M., Halbeek, H. van, Robert G. Bergman, A. & Bertozzi, C. R. Mechanistic Investigation of the Staudinger Ligation. (2005). doi:10.1021/JA044461M
3. McKay, C. S. & Finn, M. G. Click Chemistry in Complex Mixtures: Bioorthogonal Bioconjugation. *Chem. Biol.* **21,** 1075–1101 (2014).
4. Kolb, H. C., Finn, M. G. & Sharpless, K. B. Click Chemistry: Diverse Chemical Function from a Few Good Reactions. *Angew. Chem. Int. Ed. Engl.* **40,** 2004–2021 (2001).
5. Himo, F. *et al.* Copper(I)-Catalyzed Synthesis of Azoles. DFT Study Predicts Unprecedented Reactivity and Intermediates. *J. Am. Chem. Soc.* **127,** 210–216 (2004).
6. Agard, N. J., Prescher, J. A. & Bertozzi, C. R. A Strain-Promoted [3 + 2] Azide–Alkyne Cycloaddition for Covalent Modification of Biomolecules in Living Systems. *J. Am. Chem. Soc.* **126,** 15046–15047 (2004).
7. Blackman, M. L., Royzen, M. & Fox, J. M. Tetrazine Ligation: Fast Bioconjugation Based on Inverse-Electron-Demand Diels–Alder Reactivity. *J. Am. Chem. Soc.* **130,** 13518–13519 (2008).
8. Devaraj, N. K., Weissleder, R. & Hilderbrand, S. a. Tetrazine-Based Cycloadditions : Application to Pretargeted Live Cell Imaging Tetrazine-Based Cycloadditions : Application to Pretargeted Live Cell Imaging. *Communications* **19,** 2297–2299 (2008).
9. Darko, A. *et al.* Conformationally Strained trans-Cyclooctene with Improved Stability and Excellent Reactivity in Tetrazine Ligation. *Chem. Sci.* **5,** 3770–3776 (2014).
10. Sauer, J. *et al.* 1,2,4,5-Tetrazine: Synthesis and Reactivity in [4+2] Cycloadditions. *European J. Org. Chem.* **1998,** 2885–2896 (1998).
11. Versteegen, R. M., Rossin, R., Ten Hoeve, W., Janssen, H. M. & Robillard, M. S. Click to release: Instantaneous doxorubicin elimination upon tetrazine ligation. *Angew. Chemie - Int. Ed.* **52,**

14112–14116 (2013).

12.   Fan, X. *et al.* Optimized Tetrazine Derivatives for Rapid Bioorthogonal Decaging in Living Cells Angewandte. 1–6 (2016). doi:10.1002/anie.201608009

13.   Taylor, M. T., Blackman, M. L., Dmitrenko, O. & Fox, J. M. Design and Synthesis of Highly Reactive Dienophiles for the Tetrazine– *trans-* Cyclooctene Ligation. *J. Am. Chem. Soc.* **133,** 9646–9649 (2011).

14.   Blackman, M. L., Royzen, M. & Fox, J. M. Tetrazine ligation: Fast bioconjugation based on inverse-electron-demand Diels-Alder reactivity. *J. Am. Chem. Soc.* **130,** 13518–13519 (2008).

15.   Liu, F., Liang, Y. & Houk, K. N. Theoretical Elucidation of the Origins of Substituent and Strain Effects on the Rates of Diels–Alder Reactions of 1,2,4,5-Tetrazines. *J. Am. Chem. Soc.* **136,** 11483–11493 (2014).

16.   Kronister, S., Svatunek, D., Denk, C. & Mikula, H. Acylation-Mediated 'Kinetic Turn-On' of 3-Amino-1,2,4,5-tetrazines. *Synlett* **29,** (2018).

17.   Peri, F., Cipolla, L. & Nicotra, F. Tin-mediated regioselective acylation of unprotected sugars on solid phase. *Tetrahedron Lett.* **41,** 8587–8590 (2000).

18.   Yang, J., Karver, M. R., Li, W., Sahu, S. & Devaraj, N. K. Metal-Catalyzed One-Pot Synthesis of Tetrazines Directly from Aliphatic Nitriles and Hydrazine. *Angew. Chemie Int. Ed.* **51,** 5222–5225 (2012).

19.   Mayer, S. & Lang, K. Tetrazines in Inverse-Electron-Demand Diels–Alder Cycloadditions and Their Use in Biology. *Synthesis (Stuttg).* **49,** 830–848 (2016).

20.   Lang, K. *et al.* Genetic Encoding of Bicyclononynes and *trans* -Cyclooctenes for Site-Specific Protein Labeling in Vitro and in Live Mammalian Cells via Rapid Fluorogenic Diels–Alder Reactions. *J. Am. Chem. Soc.* **134,** 10317–10320 (2012).

21.   Boutureira, O. & Bernardes, G. J. L. Advances in Chemical Protein Modification. *Chem. Rev.* **115,** 2174–2195 (2015).

22.   Pinner, A. Ueber die Einwirkung von Hydrazin auf die Imidoäther. *Berichte der Dtsch. Chem. Gesellschaft* **30,** 1871–1890 (1897).

23.   Wu, H., Yang, J., Šečkutė, J. & Devaraj, N. K. In Situ Synthesis of Alkenyl Tetrazines for Highly Fluorogenic Bioorthogonal Live-Cell Imaging Probes. *Angew. Chemie Int. Ed.* **53,** 5805–5809 (2014).

24.   Haun, J. B., Devaraj, N. K., Hilderbrand, S. A., Lee, H. & Weissleder, R. Bioorthogonal chemistry amplifies nanoparticle binding and enhances the sensitivity of cell detection. *Nat. Nanotechnol.* **5,** 660–5 (2010).

25.   Hong, S., Carlson, J., Lee, H. & Weissleder, R. Bioorthogonal Radiopaque Hydrogel for Endoscopic Delivery and Universal Tissue Marking. *Adv. Healthc. Mater.* **5,** 421–426 (2016).

26.   Takimoto, H.H., Denault G.C.. 3-Amino-s-tetrazines from the thermal decomposition of 4-amino-3-azido-s-triazoles. *Tetrahedron Lett.* **7,** 5369–5373 (1966).

27.   Rossin, R. *et al.* Triggered Drug Release from an Antibody-Drug Conjugate using Fast "Click-to-Release" Chemistry in Mice. *Bioconjug. Chem.* **27,** 1697–1706 (2016).

28.   Lemke, E. A. Origin of Orthogonality of Strain-Promoted Click Reactions. 12431–12435 (2015). doi:10.1002/chem.201501727

29.   Spencer, E.Y., Wright, G.F. . *J. Am. Chem. Soc.* **63,** 1281–1285 (1941).

30.   Tsourlakis, M.C.; Klein, F.; Kluth, M.; Quaas, A.; Graefen, M.; Haese, A.; Simon, R.; Sauter, G.; Schlomm, T.; Minner, S. PSMA expression is highly homogenous in primary prostate cancer. *Appl. Immunohistochem. Mol. Morphol.* **24,** 449–455 (2015).

31.   Peng, Z.H.; Sima, M.; Salama, M.E.; Kopeckova, P.; Kopecek, J. . Spacer length impacts the efficacy of targeted docetaxel conjugates in prostate-specific membrane antigen expressing prostate cancer. *J. Drug. Target.* **21,** 968–980 (2013).

32. Zhang, H. *et al.* A Novel Prostate-Specific Membrane-Antigen (PSMA) Targeted Micelle-Encapsulating Wogonin Inhibits Prostate Cancer Cell Proliferation via Inducing Intrinsic Apoptotic Pathway. *Int. J. Mol. Sci.* **17,** 676 (2016).

33. Matsumura, Y. . M. H. A new concept for macromolecular therapeutics in cancer chemotherapy: mechanism of tumoritropic accumulation of proteins and the antitumor agent smancs. *Cancer Res.* **46,** 6387–6392 (1986).

34. Bertrand, N., Wu, J., Xu, X., Kamaly, N. & Farokhzad, O. C. Cancer nanotechnology : The impact of passive and active targeting in the era of modern cancer biology ☆. *Adv. Drug Deliv. Rev.* **66,** 2–25 (2014).

35. Miller, M. A. *et al.* chemistry. *Nat. Commun.* **8,** 1–13 (2017).

36. Miller, M. A. *et al.* Modular Nanoparticulate Prodrug Design Enables Efficient Treatment of Solid Tumors Using Bioorthogonal Activation. *ACS Nano* acsnano.8b07954 (2018). doi:10.1021/acsnano.8b07954

37. Ogundele, O. M. *et al.* Basic Principles of Fluorescence Microscopy. (2013).

38. Horoszewicz J Leong S Kawinski E Karr J Rosenthal H Chu T Mirand E Murphy G. LNCaP model of human prostatic carcinoma. *Cancer Res.* **43,** 1809–1818 (1983).

39. Kaighn, M. E. . N. K. E. . O. Y. . L. J. F. . J. L. W. . Establishment and characterization of a human prostatic carcinoma cell line (PC-3). *Invest. Urol.* **17,** 16–23 (1979).

40. Scientific, T. F. Presto Blue Cell Viablity Reagent. Available at: https://www.thermofisher.com/order/catalog/product/A13261.